

# Resolved complex coastlines and land–sea contrasts in a high-resolution regional climate model: a comparative study using prescribed and modelled SSTs

By TIAN TIAN<sup>1\*</sup>, FREDRIK BOBERG<sup>1</sup>, OLE BØSSING CHRISTENSEN<sup>1</sup>, JENS HESSELBJERG CHRISTENSEN<sup>1</sup>, JUN SHE<sup>1</sup> and TIMO VIHMA<sup>2</sup>,

<sup>1</sup>Danish Meteorological Institute, Lyngbyvej 100, 2100 Copenhagen, Denmark; <sup>2</sup>Finnish Meteorological Institute, P.O. Box 503, 00101 Helsinki, Finland

(Manuscript received 13 November 2012; in final form 28 June 2013)

## ABSTRACT

We configured a coupled model system, comprising a regional climate model (RCM) and a regional ocean model, for the North Sea and Baltic Sea region at 6 nm resolution. A two-way nested fine-grid (1 nm) ocean domain is for the first time included for the Danish coastal waters in coupled RCMs to resolve the water exchange between the two regional seas. Here, we (1) assess the sensitivity of the near-surface atmosphere to prescribed sea surface temperatures (SSTs) from the European Centre for Medium-Range Weather Forecasts (ECMWF) ERA-Interim (ERA-I) reanalysis and those modelled by the coupled system, and (2) examine different ocean responses in coarse and fine grids to atmospheric forcing. The experiments were performed covering the years 1990–2010, both using ERA-I lateral boundary conditions. ERA-I SSTs generally agree well with satellite SSTs in summer with differences within 1°C, but the ERA-I overestimates the ice extent by 72% in winter due to the coarse resolution in the Baltic Sea. The atmosphere in the Baltic land–sea transition was more sensitive to high-resolution modelled SSTs with a significant improvement in winter, but it also provided a cold bias in summer as a combination of errors from both atmospheric and ocean models. Overall, the coupled simulation without observational constraints showed only minor deviations in the air–sea interface in the Baltic coastal region compared to the prescribed simulation, with seasonal mean differences within 2°C in 2 m air temperatures and 1°C in SSTs. An exception was in the Danish water, where the fine-grid ocean model yielded a better agreement with SST measurements and showed a smaller difference between the two simulations than the coarse-grid ocean model did. In turn, the modification on the atmosphere induced by modelled SSTs was negligible. The atmospheric–ocean–ice model in this configuration was found capable of reproducing the observed interannual variability of SST and ice extent in the Baltic Sea as well as the monthly extreme wind speeds and sea levels on a local scale for Denmark during the period 1990–2010. This article provides the first results in an attempt to resolve the Danish coasts with this accuracy in an RCM as a first step towards a fully coupled system for the region of interest.

**Keywords:** RCM, Baltic Sea, Danish coasts, sea surface temperature, sea ice

## 1. Introduction

Dynamic downscaling with high-resolution regional climate models (RCMs) has been shown to add value to global atmosphere–ocean general circulation model (GCM) results by providing better regional details (Christensen and Christensen, 2003). However, the quality of RCMs strongly

relies on the accuracy of the boundary forcing (including sea surface conditions) from the GCMs (Rummukainen, 2010). This poses an inevitable limitation on the dynamic downscaling of climate in the region surrounding the Baltic area as both sea surface temperatures (SSTs) and sea ice conditions are subject to substantial bias, particularly due to limited resolution in the ocean model component in GCMs (Meier, 2006; Neumann, 2010).

The coupling to a regional ocean model has the advantage in providing SST and sea ice with high resolution in time and space in a consistent way (Gustafsson et al., 1998).

\*Corresponding author.  
email: tian@dmi.dk

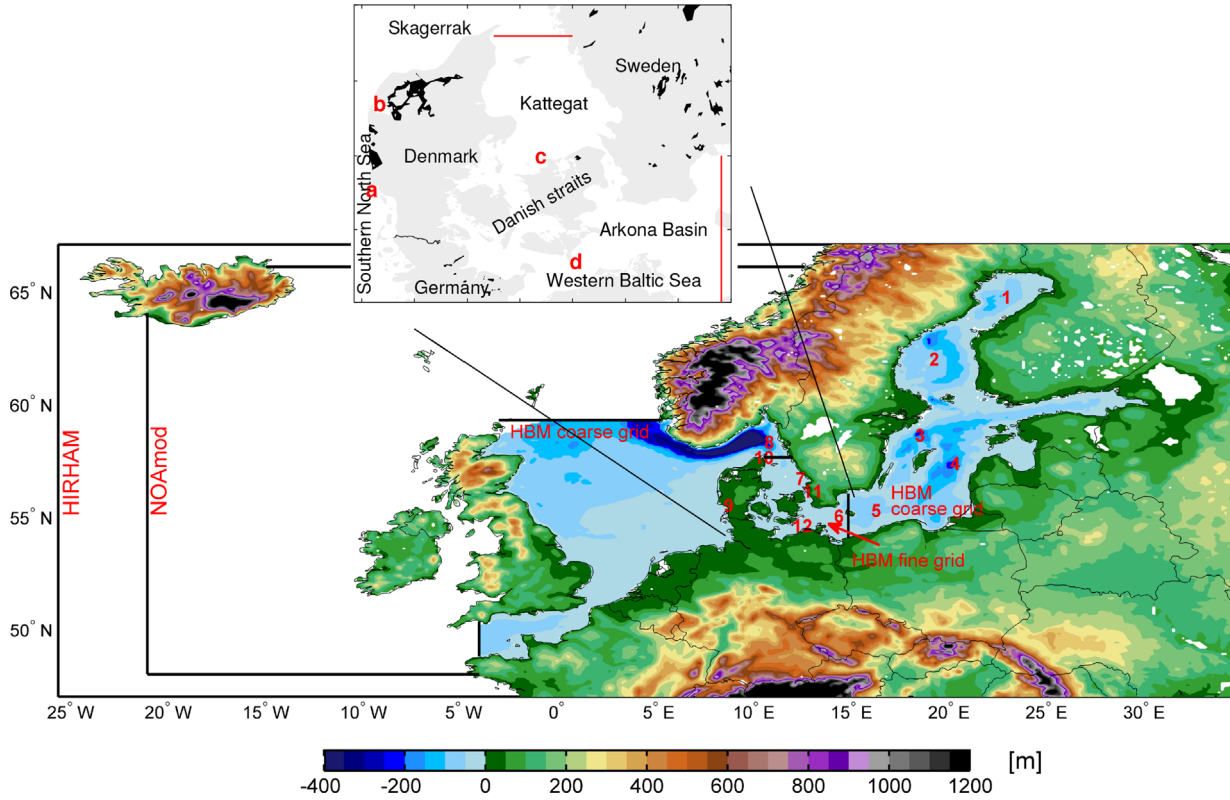


*Fig. 1.* Topography of model areas: HIRHAM – the regional atmospheric model covering the entire area; NOAmod – the surge model covering the northeast Atlantic Ocean and the North Sea (NS), enclosed by the black lines; HBM coarse grid – the regional ocean model covering the North Sea, with open boundaries at 59.25°N and 4.08°W, and the Baltic Sea; and HBM fine grid – the transition zone including the Kattegat, the Danish straits and the Arkona Basin (AB) (indicated in the inset figure), two-way nested with the outer model. Details of model grids are listed in Table 1. Positions for SST stations are indicated by numbers: 1, Bothnian Bay; 2, Bothnian Sea; 3, Landsort; 4, East Gotland Basin; 5, Bornholm Basin; 6, Arkona; 7, Kattegat; and 8, Skagerrak. Positions for tide gauges are indicated by numbers: 9, Esbjerg; 10, Hirtshals; 11, Hornbæk; and 12, Gedser. Positions for land wind stations are indicated in the inset figure by a, Blåvandshuk; b, Thyborøn; c, Griben; and d, Gedser. Stations coordinates are listed in Table 2.

Regional coupled atmosphere–ocean–ice models for the North Sea and the Baltic Sea have been developed over the last two decades for short-range seasonal forecasting and for simulating future climate change (Gustafsson et al., 1998; Hagedorn et al., 2000; Döscher et al., 2002; Schrum et al., 2003; Lehmann et al., 2004). However, the complex land–sea contrast around Denmark is not well resolved, even with state-of-the-art coupled regional ocean–atmosphere models (see e.g. Fig. 1). The role of the sea around Denmark as a controlling mechanism of certain local weather events (e.g. land–sea breeze and sensitivity to sea ice coverage) is therefore poorly represented by current RCMs (Jacob et al., 2007; Lucas-Picher et al., 2012). The consistency of regional SSTs and ice concentrations with the regional climate around Denmark in a climate change experiment is potentially improved using a coupled model system. Therefore, it has become a central topic to validate such a model in a way that

addresses a central question to downscaling: Will this consistency introduce new limitations due to the added complexity to the model system?

Dynamical downscaling, when driven by observation-based conditions at the lateral boundaries, is meant to simulate weather events as they may develop when driven by the most ideal boundary conditions, but this is only in a statistical sense, without necessarily expecting the timing or amplitude of these events to agree with the driving conditions (e.g. Rummukainen, 2010). Complete consistency within the modelling domain can be ensured, for example through spectral nudging (von Storch et al., 2000). Therefore, one of the methods to assess the quality of such simulations is to analyse higher order statistics of central variables in the simulation rather than to compare the sequence of events per se. This was an essential outcome of the ENSEMBLES project where different methods to assess model quality have been analysed in depth (see e.g.

Christensen et al., 2010; Kjellström and Giorgi, 2010, and references therein). In this work, this approach to analyse model performance has been adopted.

Due to its location in the transition zone between continental and maritime climates, the Baltic Sea is exceptionally vulnerable to climate change (BACC, 2008). The presence of coastlines and islands causes divergent motions in the upper layers of the sea and often causes rapid changes in SST and the sea ice cover (Gustafsson et al., 1998). These specific geometrical features, in turn, influence the climate in the Baltic Sea. The circulation in the Baltic Sea basically consists of a surface current with brackish water, which flows out from the Baltic through the Kattegat to the Skagerrak and the North Sea, and an undercurrent with saline water, which flows in the opposite direction. Between the brackish and saline waters, there is a permanent halocline. Above the halocline, vertical mixing is driven by wind and thermal convection. The near-bottom inflow from the North Sea is a major source of deep-water renewal in the Baltic Sea and a key indicator of the state of the physical–biogeochemical system (Meier and Kauker, 2003; Meier, 2006; Neumann, 2010). It is well known that bathymetry in the Danish straits and the western Baltic Sea is one of the governing factors for water exchange between these two regional seas (Bendtsen et al., 2009; Burchard et al., 2009; Hofmeister et al., 2011). Also, previous studies have demonstrated that a spatial resolution of at least 1 nm is necessary to realistically describe topographic features like sills, sounds, and coastlines in the Danish straits (She et al., 2007; Hofmeister et al., 2011). This necessitates the development of a high-resolution RCM, which makes it possible to resolve both large-scale processes in the Baltic Sea and local conditions around Denmark (Larsen et al., 2013).

We configured a coupled model system, comprising an RCM and a 3D ocean circulation model, for the North Sea and Baltic Sea region in 6-nm resolution. A two-way nested fine-grid ocean domain is included for the first time in the coupled RCMs, which allows for a resolution of 1 nm in the transition zone and gives improved description of the transitional water (She et al., 2007). The RCM has been extensively used for the European region to downscale variability and climate change signals from global models, for instance during the PRUDENCE (Prediction of Regional Scenarios and Uncertainties for Defining European Climate Change Risks and Effects) project (Christensen and Christensen, 2007). More recently, sensitivity analyses on the effect of domain size and resolution on simulated precipitation and temperature have been conducted with this RCM, and the setup used in this study was demonstrated to provide superior agreement with an observational data set covering Europe and Denmark on a seasonal basis (Larsen et al., 2013). In principle, both models with their configurations have great advantages in

long-term simulations in the region of interest regarding the computational costs due to the domain size and high resolution versus the benefit of the added accuracy.

The main scope of this study is to investigate the sensitivity of the near-surface atmosphere to the representation of SSTs in different resolutions and to identify the different ocean responses in coarse and fine grids to atmospheric forcing on multi-year time scales in the coupled system. This is a necessary step towards the development of a fully coupled high-resolution regional ocean–atmosphere model for Northern Europe. We performed two RCM experiments for 1990–2010 by using lateral boundary conditions from the ERA-Interim (ERA-Interim) reanalysis project (Dee et al., 2011) from the European Centre for Medium-Range Weather Forecasts (ECMWF). The difference between the two simulations was the choice of SST inputs to the RCM either from the ocean model without observational constraints on the regional scale or from the lower resolution ERA-Interim reanalysis data of observed climate. The evaluation of these two simulations against observations enabled us to (1) assess the quality of sea surface conditions from the reanalysis data and the improvement by applying the high-resolution modelled SSTs, and (2) define the added value of the nested fine-grid ocean domain in the coupled system. Furthermore, this work provides a first attempt to resolve the Danish coasts with this accuracy in RCM downscaling. It also serves as a knowledge basis for the development of a fully (flux) coupled system with a special interest in the area around Denmark.

## 2. Methods

### 2.1. The RCM

The RCM used in this study is HIRHAM5 (Christensen et al., 2006), which is a hydrostatic RCM developed at the Danish Meteorological Institute (DMI). The HIRHAM model is based on the dynamical core of the HIRLAM7 (High Resolution Limited Area Model) weather forecasting model (Eerola, 2006) and the physical core of the ECHAM5 GCM (Roeckner et al., 2003) using the Tiedtke (1989) mass flux convection scheme, with modification after Nordeng (1994) and Sundqvist (1978) microphysics. The land surface scheme is unmodified from that used in the ECHAM5 model (Roeckner et al., 2003), which employs the rainfall-runoff scheme described in the work of Dumenil (1992). A dynamical downscaling is performed with the RCM nested into the ERA-Interim reanalysis data at a resolution of  $\sim 80$  km (T255). The zonal and meridional wind components, temperature and specific humidity at all atmospheric model levels as well as surface pressure fields are introduced to the RCM as forcing at the lateral boundaries at 6-h intervals. In a standard run, SST fields

from ERAI are interpolated and prescribed to the RCM once per day. Significant errors are possibly introduced by its low resolution in the land–sea transition, especially in the Danish straits and the northern Baltic Sea (Gustafsson et al., 1998).

## 2.2. The regional ocean model

The ocean model used in this study is the High-Resolution Operational Model for the Baltic (HIROMB)-Baltic Operational Oceanographic System (BOOS) model (HBM), which has been well calibrated for the Baltic Sea both for operational services (Berg, 2012; Wan et al., 2012) and for long-term reanalysis (Fu et al., 2012). HBM is a 3D, baroclinic circulation model that uses the hydrostatic and Boussinesq assumptions. The primitive equations are discretised on an Arakawa C-grid. The mixing scheme applied is based on the  $k$ - $w$  turbulence model (Umlauf et al., 2003; Berg, 2012). The model also includes a simplified sea ice module treating both the dynamics and thermodynamics (Kleine and Sklyar, 1995).

The model surface is forced by hourly RCM outputs of 10 m wind, 2 m air temperature, mean sea level pressure, specific humidity and cloud cover. The surface heat flux is parameterised using bulk quantities of both lower atmosphere and upper ocean or sea ice, respectively (Liu et al., 1979). At the open model boundaries in the North Sea and in the English Channel, the model is forced by tides, surges and lateral temperatures and salinity fields. Surges are calculated from a northeast Atlantic barotropic surge model (NOAmod), also driven by the RCM. The tidal sea level is derived from 17 major tidal constituents. The density profile is derived from International Council for the Exploration of the Sea (ICES) T/S monthly climatology (Janssen et al., 1999) and interpolated over time; a sponge layer acts as a buffer zone between the inner model domain and the prescribed T/S boundary values. The reflection and absorption of shortwave radiation by the seabed in shallow zones are prescribed as a thermodynamic bottom boundary condition. The ocean model includes river runoff from 79 rivers, either from real-time measurements for the major rivers in the North Sea (provided by the Bundesamt für Seeschifffahrt und Hydrographie, or BSH) or as calculated with a large-

scale hydrological model for the Baltic Sea runoff (Graham, 1999, provided by the Swedish Meteorological and Hydrological Institute, or SMHI).

## 2.3. Model configurations

The HBM has two model configurations (Fig. 1 and Table 1): an outer model for the North Sea-Baltic Sea and an inner model for the transition area, with horizontal resolutions of 6 and 1 nm, respectively. The time steps of the outer and inner model are 90 and 45 s, respectively. In the model interface on each side of the border, the hydrodynamic parameters are computed and interactively coupled, which allows for a nested grid with a high resolution to interact with a coarser grid (Berg and Poulsen, 2012). Both models are set up horizontally in spherical coordinates and vertically in  $z$  coordinates. The outer model has a maximum of 50 vertical layers with a thickness of 8 m in the surface layer (to avoid drying at low tides) and 2 m between the depths of 8 and 80 m. Below 80 m, the layer thickness increases gradually from 4 to 50 m. The inner model has a maximum of 52 vertical layers with a thickness of 2 m in the surface layer, 1 m between the depths of 2 and 30 m and 2 m for the deeper layers below 30 m.

The HIRHAM and NOAmod models are configured with the same horizontal resolution of 6 nm, but they cover different areas (Fig. 1) so that NOAmod can provide surge boundary conditions for HBM while HIRHAM provides meteorological forcing for the ocean models. The HIRHAM grid is set to match the coarse grid of HBM where they overlap, so that interpolation is avoided when exchanging information between them. It is, however, necessary to provide HIRHAM with lower resolution surface fields from ERAI for the ocean areas outside of the HBM domain.

## 2.4. Experiments

We performed two HIRHAM simulations for the period 1990–2010. In the standard run, HIRHAM was driven by the global meteorological reanalysis products from ERAI on the lateral boundaries and with prescribed SSTs also from ERAI. In the other simulation, HBM was coupled to HIRHAM to provide modelled SST fields with a higher resolution. The idea of the coupling was to exchange fields

Table 1. Regional atmosphere and ocean model grids

Model	Domain	Resolution (latitude $\times$ longitude)	Vertical levels
HIRHAM	25.64°W–34.64°E, 46.95°N–67.05°N	6' $\times$ 10'	31
NOAmod	21.08°W–13.08°E, 47.95°N–66.05°N	6' $\times$ 10'	1
HBM coarse grid	4.08°W–30.25°E, 48.55°N–65.85°N	6' $\times$ 10'	50
HBM fine grid	9.35°E–14.82°E, 53.59°N–57.59°N	1' $\times$ 1'40"	52

between HIRHAM and HBM. The HIRHAM-HBM coupler worked in a sequential fashion, with HIRHAM first integrating for 1 d and providing hourly forcing fields to HBM. Then HBM integrated for 1 d and delivered the SST field to HIRHAM for the next day. Various coupling intervals can be specified in the coupler, typically 3 h, 24 h or 120 h, depending on the interaction time lengths of interest (Masson et al., 2012). In the experiment discussed in this article, 24 h coupling was used because this time interval of reading the SST field was used in the standard run.

In both cases, HBM was forced hourly by HIRHAM output. The ocean's initial conditions were taken from a standard simulation of a 50 yr hindcast experiment from 1960 to 2009 (Fu et al., 2012). Both the ocean and the atmospheric model simulations started on 1 January 1989, where the initial year was used for spin-up. The analysed period is 1990–2010.

## 2.5. Database

Satellite bulk SSTs for the simulation period were taken from the BSH Baltic product, where monthly means were computed with the MCSST algorithm for National Oceanic and Atmospheric Administration (NOAA) Advanced Very High Resolution Radiometer night-time observations (Høyer and She, 2004). Sea ice is assumed to be present when missing values occur from December to May. The SST is then set to the approximate freezing point of  $-0.3^{\circ}\text{C}$ . For model validation, the satellite SST data were transformed to the model grid using a nearest neighbour interpolation. Furthermore, in situ SST measurements for the period 2000–2010 were obtained from the SMHI database SHARK (Svenskt HavsARKiv). Eight stations

were selected spanning from Skagerrak and Kattegat to the southern and northern Baltic Sea (Fig. 1 and Table 2).

Annual maximum ice extent (MIB) of the Baltic Sea is published in Vihma and Haapala (2009). The longest available data set of daily (or every 3 d) sea ice concentrations is found in the archive of lower boundary conditions utilised in the weather forecasting model HIRLAM. The data are based on digitisation of Finnish Meteorological Institute (FMI) operational ice charts, which had 3 d intervals in the early 2000s but later covered every day. The resolution of the data is  $0.17^{\circ}$  in latitude and usually  $0.33^{\circ}$  in longitude. In the period October 2000–December 2002, the southernmost limit was  $58.0^{\circ}\text{N}$ , but from January 2003 onwards it was  $57.0^{\circ}\text{N}$ . In order to address the same region for the whole period from 2000, we had to set the southernmost limit at  $58.0^{\circ}\text{N}$ . We calculated the modelled and observed ice extent and total ice area in the northern part of the Baltic Sea (NBS,  $58.0\text{--}65.8^{\circ}\text{N}$ ,  $17.17\text{--}30.17^{\circ}\text{E}$ ), starting from 30 October 2000 and ending on 31 December 2010. The total ice area is defined as the sum of each grid-cell area multiplied by the ice concentration in that cell, whereas the ice extent is defined as the sum of all grid-cell areas with an ice concentration of at least 10%. This is the World Meteorological Organization practice, which is also applied in the Baltic Sea to FMI and SMHI observations. However, the observational estimate for the NBS is not absolutely accurate due to data gridding; in coastal regions, the domain did not exactly match the meandering shape of the coastline. The uncertainty is of the order of 5–10%.

To evaluate the simulated extreme storm events and highest sea levels at the Danish coasts, hourly tidal gauge records and 10-min average readings of wind speeds were obtained from a DMI database. The water level stations at

Table 2. Station list (locations are indicated in Fig. 1)

Station number	Name	Latitude	Longitude	Period	Measurements (frequency)
1	F9	$64.71^{\circ}\text{N}$	$22.07^{\circ}\text{E}$	2000–2010	SST (1–2 times per month)
2	C3	$62.66^{\circ}\text{N}$	$18.95^{\circ}\text{E}$	2000–2010	SST (once per month)
3	BY31	$58.58^{\circ}\text{N}$	$18.23^{\circ}\text{E}$	2000–2010	SST (1–4 times per month)
4	BY15	$57.33^{\circ}\text{N}$	$20.05^{\circ}\text{E}$	2000–2010	SST (once per month)
5	BY05	$55.25^{\circ}\text{N}$	$15.98^{\circ}\text{E}$	2000–2010	SST (1–2 times per month)
6	BY02	$55.00^{\circ}\text{N}$	$14.08^{\circ}\text{E}$	2000–2010	SST (1–2 times per month)
7	Anholt E	$56.67^{\circ}\text{N}$	$12.12^{\circ}\text{E}$	2000–2010	SST (1–3 times per month)
8	Å17	$58.28^{\circ}\text{N}$	$10.51^{\circ}\text{E}$	2000–2010	SST (1–2 times per month)
9	Esbjerg	$55.47^{\circ}\text{N}$	$8.43^{\circ}\text{E}$	1990–2005	Water level (hourly)
10	Hirtshals	$57.60^{\circ}\text{N}$	$9.97^{\circ}\text{E}$	1990–2005	Water level (hourly)
11	Hornbæk	$56.10^{\circ}\text{N}$	$12.47^{\circ}\text{E}$	1990–2005	Water level (hourly)
12	Gedser	$54.57^{\circ}\text{N}$	$11.93^{\circ}\text{E}$	1990–2005	Water level (hourly)
a	Blåvandshuk	$55.56^{\circ}\text{N}$	$8.08^{\circ}\text{E}$	1990–2010	Wind speed (10-min average)
b	Thyborøn	$56.71^{\circ}\text{N}$	$8.22^{\circ}\text{E}$	1990–2010	Wind speed (10-min average)
c	Gniben	$56.01^{\circ}\text{N}$	$11.28^{\circ}\text{E}$	1990–2010	Wind speed (10-min average)
d	Gedser	$54.57^{\circ}\text{N}$	$11.94^{\circ}\text{E}$	1994–2010	Wind speed (10-min average)

Esbjerg and Hirtshals were chosen to represent the North Sea coast, and the stations at Hornbæk and Gedser were chosen to represent the transition zone (Fig. 1 and Table 2). When considering wind, the land stations at Blåvandshuk and Thyborøn were chosen to represent the North Sea coast, and the stations at Griben and Gedser were chosen to represent the transition zone (Fig. 1 and Table 2). Both water level and wind speed data were used to derive monthly means and monthly maxima. Some discrepancies in wind speed comparison are inevitable due to different resolutions in time (an instantaneous model output representing a time step of 3 min, versus 10-min average observational readings of wind speeds) and in space (a land station versus a grid point with a resolution of  $\sim 11$  km). Previous studies have indicated that the HIRHAM winds over open sea are quite realistic (Rockel and Woth, 2007).

### 2.6. Ocean model validation

Fu et al. (2012) present a full validation of a standard simulation (1990–2009). They found that modelled salinity is about 0.5 psu lower than observations in the Baltic Sea, with a more prominent bias below 60 m in the central Baltic Sea. This underestimation is primarily caused by the coarse vertical grid below 175 m with a depth increment of 50 m, which introduced errors in the initialisation and also reduced the effects of saline water inflow in the bottom layer (Wan et al., 2012). The quality of modelled sea levels was also assessed by Fu et al. (2012) with tide gauge data from five stations in the Baltic Sea and nine stations in the transition area on a monthly basis. The modelled water level generally fitted well with measurements ( $R \geq 0.68$  and  $0.06 \leq \text{RMSE} \leq 0.09$  m). There is an exception at Rodby station (54.65°N, 11.35°E) with a correlation of 0.54 and an RMSE of 0.10 m. This misfit is presumably due to the station's location near the Darss Sill, where the sub-grid scale feature of narrow transport cannot be fully resolved even at a resolution of 1 nm in the nested model.

On a yearly basis, the model is capable of describing the average salinity stratification in the section from the Sound to the Gulf of Finland (GF) (Fig. 2). Between the Arkona Basin (AB) and Bornholm Sea (BS), there is a vertical incline in salinity from 8 to 10 psu within 20 m depth. This halocline further strengthens between 50 and 70 m below the surface in the East Gotland Basin and propagates into the GF (Leppäranta and Myrberg, 2009). The modelled annual average transport through the Danish straits is an outflow of  $14,000 \pm 3000 \text{ m}^3 \text{ s}^{-1}$ , in close agreement with the long-term mean freshwater supply of  $15,000 \text{ m}^3 \text{ s}^{-1}$  to the Baltic Sea (Leppäranta and Myrberg, 2009).

In this article, we first investigate the possible errors in the surface atmospheric conditions introduced by different

resolutions of SST field in the land–sea transition and the ocean response. Second, we identify added values of the two-way nested model in the transition zone to the regional coupled ocean–atmosphere model, and then assess its significance on a climate-relevant time scale. We do not show salinity differences between the two simulations because the river runoff is identical in both runs and the residence time of the Baltic deep water is over 30 yr (Meier, 2007). The differences in average salinity and in annual average transport through the Danish straits between the two simulations are found negligible. Hence, we focus on significant changes in thermal dynamics and the prominent impact on the air–sea interface during the 21 yr period. A validation on modelled SST and sea ice in both the standard and coupled simulations is shown in Section 3.

## 3. Results

### 3.1. Near-surface atmospheric variables in the Baltic region

To assess atmospheric responses to different SSTs, we investigate surface variables. Significant differences between the two simulations were mostly confined to the Baltic Sea region (Fig. 3). Compared with the standard simulation, the coupled one yielded positive winter differences and negative summer differences in 2-m air temperatures, with up to  $2^\circ\text{C}$  on average for 21 yr of daily fields (Fig. 3a and b). The results were the opposite in the transition area, where the coupled model produced somewhat colder winter conditions and locally somewhat warmer summer conditions. The significant winter temperature differences in the NBS are accompanied by a slightly higher cloud cover with differences below 0.05 (Fig. 3c). As the difference in net longwave radiation is much larger than the difference in net

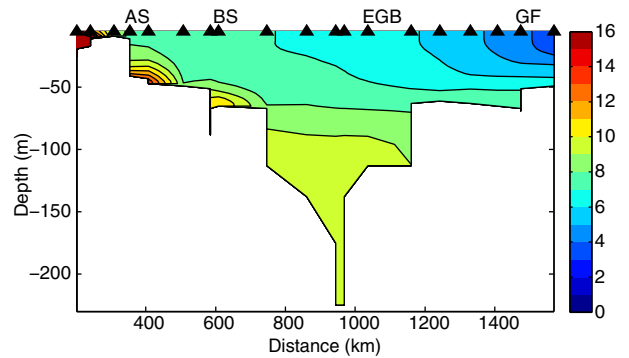


Fig. 2. Depth profile of the Baltic Sea from the Sound via the Arkona Basin (AB) and the Bornholm Sea (BS) to the Eastern Gotland Basin (EGB) and the Gulf of Finland (GF), showing the average salinity stratification from the standard simulation (1990–2010). Positions of the stations are indicated in Fig. 7.

incoming shortwave radiation (Fig. 3e and g), the cloud cover is a minor effect related to increased evaporation due to higher SSTs in the ocean model than ERAI SSTs (see Section 3.2). The negative difference in net longwave radiation indicates that the coupled run contributes more to heat fluxes at the air–sea interface over the Baltic. The relation between air temperature and other surface quantities in summer can be explained using the reverse argument (Fig. 3b, d, f and h).

We calculated spatially averaged differences (coupled minus standard simulation) in 2-m air temperatures and SSTs for the Baltic Sea. The general behaviour for December through February (DJF) and June through August (JJA) means in SSTs was similar, with less pronounced amplitudes for the atmospheric means. Overall, the absolute maximum positive and negative differences were below 1.42 and 0.38°C in 2-m air temperatures and SSTs, respectively. The DJF and JJA extremes cancelled each other out to some extent, giving a moderate variation in the annual means. To explore the seasonal variations of surface variables, we show field averages over the Baltic Sea, based on monthly means for the period 1990–2010 together with the standard deviation of the mean. The coupled run shows a higher temperature in winter and a lower temperature in summer (Fig. 4a). This is reflected by the flux components' sensible heat flux, latent heat flux and surface net longwave radiation (Fig. 4b–d). The crossover occurs between May and August. There is a slight increase in surface net shortwave radiation in March (Fig. 4e). All flux components are summarised by the net total energy, with negative values in autumn–winter (from September until March) and even more negative values in the coupled simulation (Fig. 4f). This indicates that the atmosphere received more energy from the ocean in winter and lost more energy to the ocean in summer in the coupled case than the prescribed SSTs.

### 3.2. SSTs in the Baltic Sea

The DJF and JJA mean SSTs were calculated over the simulation period and compared with satellite SSTs. A difference (model minus satellite) within 1°C is small considering uncertainties in the satellite SSTs (Löptien and Meier, 2011). The DJF means of ERAI SSTs were generally underestimated in the Baltic Sea (Fig. 5a). The significant differences exceeding  $-1^{\circ}\text{C}$  were in the deep part of the Bothnian Bay, the Bothnian Sea, the East Gotland Basin and the Bornholm Basin (Fig. 1). In contrast, the SSTs in the northern coasts of the Bothnian Bay, the GF as well as southeast Arkona were slightly overestimated by about  $1^{\circ}\text{C}$ . These biased SSTs were then used for the standard HIRHAM simulation, and the latter provided atmospheric forcing for the ocean simulation.

As a result, the spatial pattern of over- or underestimations of SST remained in the standard HBM run (Fig. 5b), with slightly smaller negative differences but larger positive differences. This indicates systematic errors with a warm bias in the Baltic Sea and a cold bias in Kattegat. Both the warm and cold biases in simulated SSTs were moderately stronger in the coupled run (Fig. 5c). This explains why 2-m air temperatures in winter showed an increase in the Baltic Sea when the relatively cold prescribed SSTs were replaced by the warmer modelled SSTs and vice versa in Kattegat (Fig. 3a). The JJA mean of ERAI SSTs generally agreed well with satellite SSTs, with differences within  $1^{\circ}\text{C}$  (Fig. 5d). In the standard simulation, a cold bias was revealed in the northeast Baltic Sea, with differences of about  $-2^{\circ}\text{C}$  (Fig. 5e). The cold bias was amplified and extended in the coupled run (Fig. 5f). This was coherent with the 2-m air temperature differences in the HIRHAM simulations in summer (Fig. 3b). The cold bias in modelled SSTs is presumably due to a depth effect of the first model layer since the mixed layer depth in summer is normally less than 10 m (Fu et al., 2012). Besides, the satellite SST has an uncertainty of  $\pm 0.5^{\circ}\text{C}$  in summer (Löptien and Meier, 2011). Overall, mean model differences relative to satellite data exceeding  $2^{\circ}\text{C}$  were rare in both simulations.

The in situ SSTs at eight stations for the period 2000–2010 were used to calculate model errors in different Baltic Sea regions (Fig. 1 and Table 2). The model results were generally in good agreement with observations: the maximum RMSEs were  $1.28^{\circ}\text{C}$  (standard) at station 2 and  $1.41^{\circ}\text{C}$  (coupled) at station 1 in the Bothnian Sea and Bothnian Bay, respectively; the minimum RMSEs were  $0.68^{\circ}\text{C}$  (standard) and  $0.82^{\circ}\text{C}$  (coupled) at station 7, Kattegat. For the standard run (relative to observations), the DJF mean SST differences were positive in the Baltic Sea (stations 1–6) but negative for the other stations in Kattegat and Skagerrak; the JJA mean differences were all negative except for station 6, Arkona; and the absolute values of the DJF and JJA mean differences were mostly below  $0.5^{\circ}\text{C}$ . For the coupled run, both DJF and JJA mean differences were somewhat amplified relative to the standard run, with absolute values below  $1^{\circ}\text{C}$ . A Taylor diagram is used to display the spatial difference of the model skills (Fig. 6). To constrain the seasonal component, we used a common method, where each month of the year was averaged over all the years in the data samples and the monthly means were subtracted from the time series of both the model and observations (Pezzulli et al., 2005). The standard simulation at stations 5–8 had a better match with observations than those in the NBS (stations 1–4) in terms of higher correlation coefficients and lower root-mean-square deviations (RMSDs). The coupled simulation showed spatial model skills close to those of the standard one, with slight deviations. A relatively poor performance was found for stations 1 and 2 in the coupled run, within the



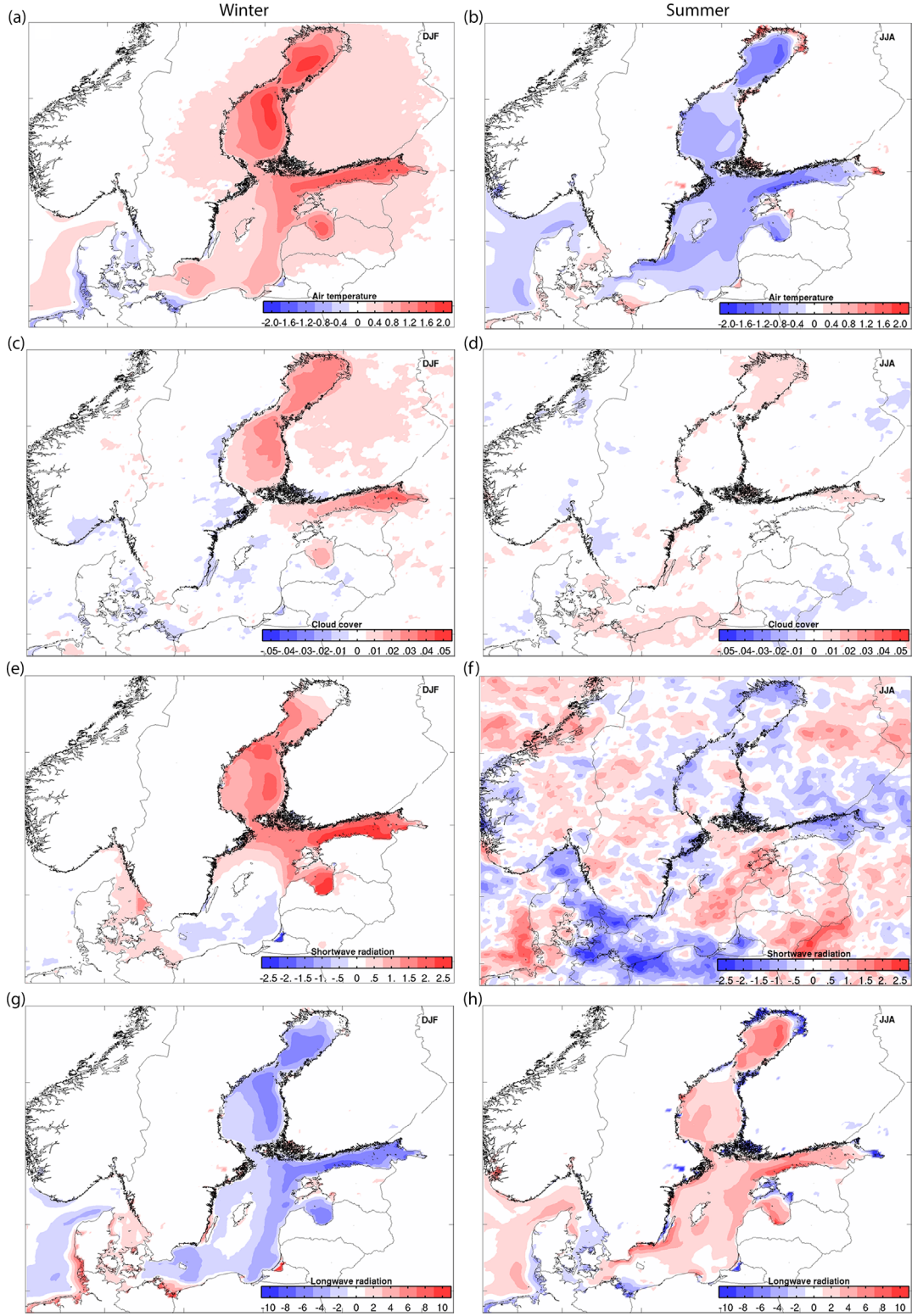


*Fig. 3.* Differences in seasonal mean (1990–2010) between the coupled and standard simulation for surface variables: 2 m air temperature in  $^{\circ}\text{C}$  (a and b), cloud cover (c and d), net incoming shortwave radiation in  $\text{W m}^{-2}$  (e and f) and net incoming longwave radiation in  $\text{W m}^{-2}$  (g and h). The left and right panels are winter (December through February, or DJF) and summer (June through August, or JJA) means, respectively.



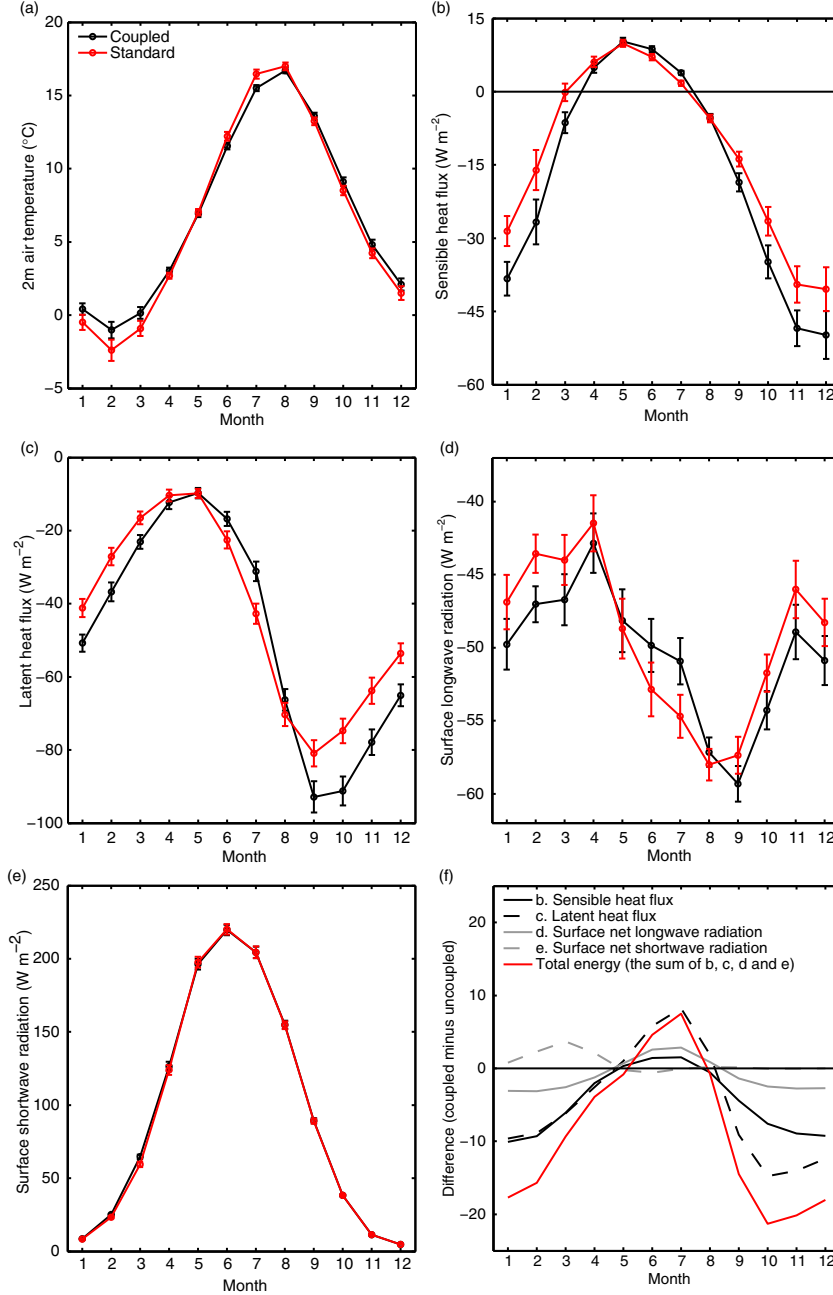


Fig. 4. Monthly means (1990–2010) with error bars for the field average over the Baltic Sea (sea points within 54–66°N, 15–30°E) for (a) 2 m air temperature; (b) sensible heat flux; (c) latent heat flux; (d) surface net longwave radiation and (e) surface net shortwave radiation, all compared for the coupled (black) and standard (red) simulation; and (f) flux differences (coupled minus prescribed simulation) for (b), (c), (d), (e) and total energy (i.e. the sum of (b)–(e)). Error bar indicates one standard error of the mean over the 21 yr. Overlap of error bars indicates that the two simulations are not significantly different.

Gulf of Bothnia. The best performance was found for stations 6 and 7 in both runs, both within the fine-grid domain.

The RMS differences of the monthly mean SST were calculated between the two simulations in order to identify the sensitivity of the ocean model to different atmospheric forcings. Significant differences were found in JJA in the

Bothnian Bay, GF and Gulf of Riga (Fig. 7), with RMS differences  $>0.6^{\circ}\text{C}$ . Generally speaking, shallow waters were more sensitive to atmospheric forcing than deep basins. Intriguingly, the shallow transition zone showed the lowest RMS differences. The relatively high RMS differences in the Arkona Sea were attributed to the

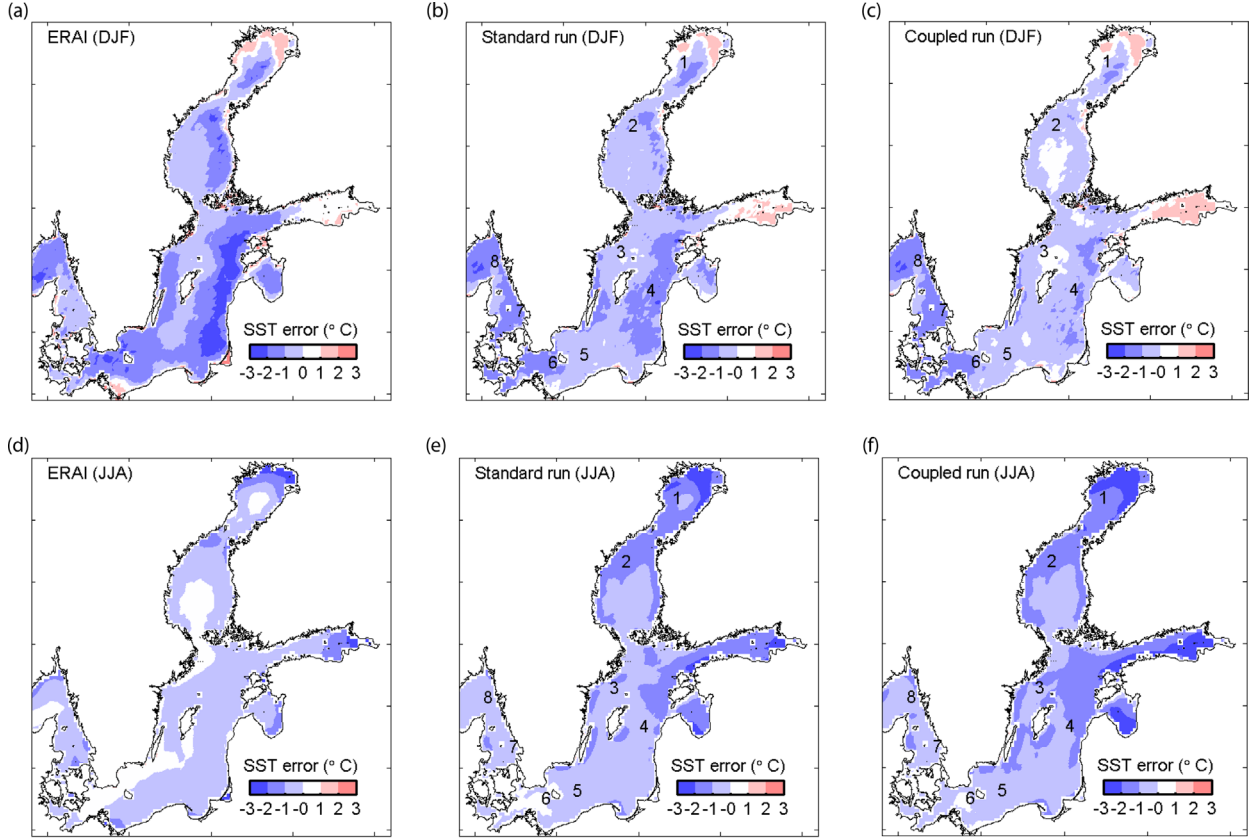


Fig. 5. Differences in seasonal mean SSTs (1990–2010) relative to satellite data. Winter (DJF) and summer (JJA) means are presented on the top and bottom panels, respectively. The results from ERAI reanalysis and from the standard and coupled run are shown from left to right, respectively. Sea ice is assumed when missing values occur in DJF in the satellite data. SST is set to the approximate freezing point of  $-0.3^{\circ}\text{C}$  where ice covered. The numbers indicate the station indices defined in Fig. 1 and Table 2 which highlight the spatial differences in model errors.

boundary effect from the coarse model domain. This pattern was coherent with the 2-m air temperature differences in the HIRHAM simulations in summer (Fig. 3b). These changes in JJA SST in the coupled simulation only cause minor differences in mixed layer depth with  $\pm 2$  m in the Baltic Sea from the standard simulation (not shown). The definition of mixed layer depth used in this study is taken from <http://www.nodc.noaa.gov/OC5/WOA94/mix.html>.

### 3.3. Sea ice in the Baltic Sea

The total observed sea ice area in the NBS ( $58.0\text{--}65.8^{\circ}\text{N}$ ,  $17.17\text{--}30.17^{\circ}\text{E}$ ) was on average 86% of the observed ice extent. This fraction not only indicates the mean ice concentration within the sea ice zone but also reflects the sensitivity of the results of the two calculation methods. The models were successful in reproducing the observed mean value; the standard run yielded 86%, the coupled run 82% and the ERAI 85%. To assess the effect of different

SSTs on modelled sea ice, the daily ice extent in the NBS was studied (Fig. 8a). The integration of the 21-yr ice extent in the coupled run showed a 33% lower value than the standard run. This substantial overestimation of ice extent in the standard run is associated with the relatively low 2-m air temperatures in winter in the prescribed HIRHAM simulation (Fig. 4a), which was caused by a 72% overestimation in the ERAI ice extent. Over the observational period (2000–2010), both the ERAI and the standard and coupled simulations were able to reproduce the interannual variation with significant correlation to observations, with  $R = 0.90, 0.92$  and  $0.93$  and  $\text{RMSE} = 7.3 \times 10^4, 3.7 \times 10^4$  and  $2.3 \times 10^4 \text{ km}^2$ , respectively. The coupled model provided the best estimate of the daily ice extent. The MIB was usually observed in February or March, as given in Fig. 8b. In the coupled run, the modelled dates matched the observed ones very well; only in 2009 did the error exceed 10 d. The date of the MIB shifted only slightly between the two simulations, except in 2003, 2009 and 2010, when the lag exceeded 1 week.

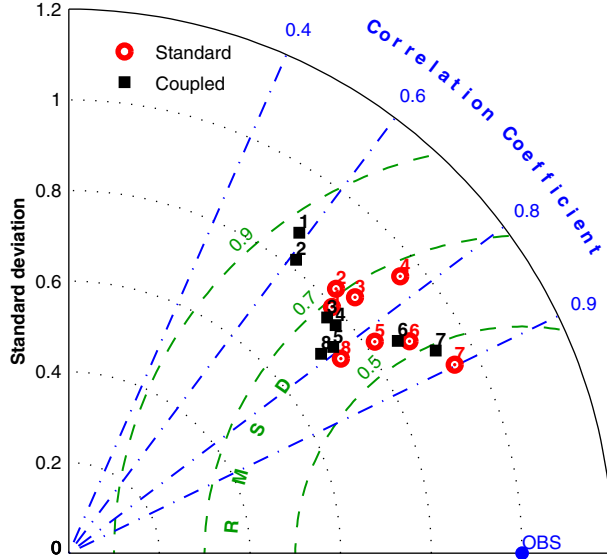


Fig. 6. Taylor diagram assessing the deseasonalised time series of SST in two simulations with correlation coefficients, normalised standard deviations and RMSDs to in situ observation (OBS). The time series from 2000 to 2010 are chosen at eight selected stations. The nearest model grid points are used, and the results are extracted according to the date of measurements. The numbers indicate the station indices defined in Fig. 5 and Table 2. The results from the coupled and standard run are indicated by black solid squares and red open circles, respectively.

The modelled sea ice distribution in the Baltic Sea at the time of the MIB was also investigated. Examples of an average winter (e.g. 2007) and an extremely mild winter (e.g. 2008) are given in Fig. 9. According to Seinä and Palosuo (1996), an average winter was defined as an MIB covering the Bothnian Bay, Bothnian Sea, GF, Gulf of Riga, northern parts of the Baltic Proper and shallow

coastal areas further south; and an extremely mild winter was defined as an MIB covering only the Bothnian Bay, part of the GF and the Bothnian Sea, and the shallow coastal area in the Gulf of Riga. Both simulations captured the main characteristics of these two different ice winters well. In the standard (prescribed) run, the ice concentration was overestimated in the Bothnian Sea and GF but very likely underestimated in the Gulf of Riga. This implies that the impact of the ERAI sea ice bias is more significant in the northern Baltic Sea. In contrast, in the coupled run, the MIB was underestimated for both years.

### 3.4. Sea level and wind speed at the Danish coasts

On an hourly basis, there are small deviations in sea level between the two simulations at the four selected stations. Both simulations have correlation coefficients, compared with hourly observations, of 0.97 and 0.89 and RMSEs of 0.17 m and 0.13 m at the North Sea coastal stations Esbjerg and Hirtshals, respectively. In the inner Danish water, the correlation coefficients were 0.89 and 0.87 at the Hornbæk and Gedser stations, respectively, and the RMSEs were 0.11 m in both occasions. To identify local effects on extreme surge events, monthly maxima of sea level were derived from hourly observations and model results (Fig. 10). Along the North Sea coast, the ocean model failed to reproduce the water level above 3 m at Esbjerg, resulting in RMSDs of 0.29 (standard) and 0.27 m (coupled); the model likely overestimated the water level at Hirtshals, with RMSDs of 0.18 m in both simulations. In the transitional water, the simulations had RMSDs of 0.18 and 0.15 m at Hornbæk and Gedser, respectively. Based on this comparison, the coupled model is unlikely to introduce a significant difference from the uncoupled model in a long-term simulation.

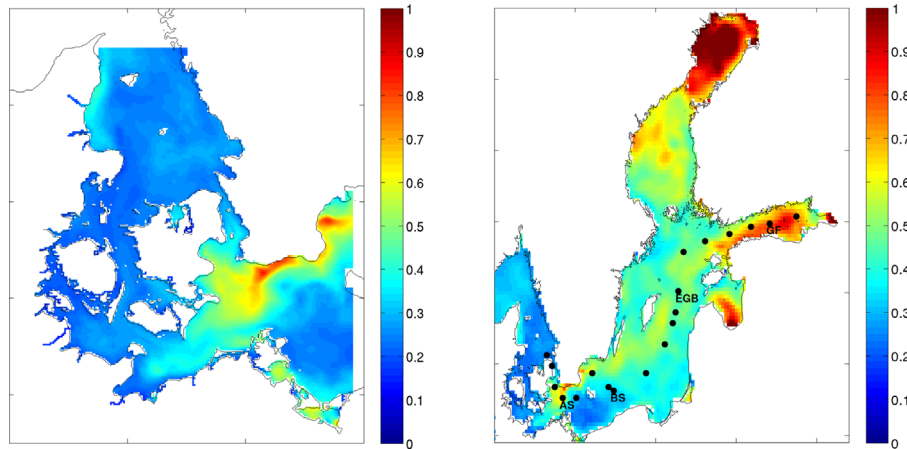


Fig. 7. RMS differences of the JJA monthly mean SST between the coupled and standard simulation in the period 1990–2010. Positions of the stations from the southwest to northeast Baltic Sea, at which a depth profile of average salinity is shown in Fig. 2.

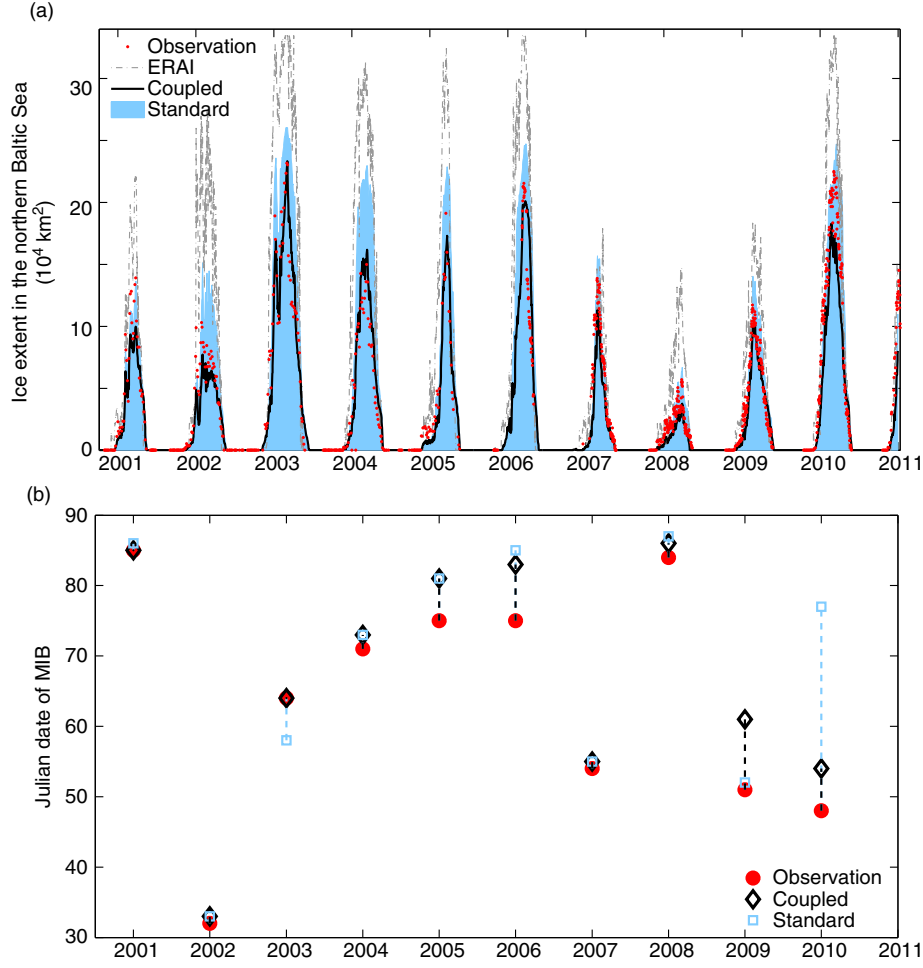


Fig. 8. (a) Daily ice extent from observations (red dots), ERAI reanalysis (grey line) and the coupled (black line) and standard (shaded area) simulations in the northern Baltic Sea (58.0–65.8°N, 17.17–30.17°E) since 30 October 2000. (b) Julian date of annual maximum ice extent (MIB) of the whole Baltic Sea from observations (red) together with the coupled (black) and standard (blue) simulations. The dashed lines between modelled and observed dates indicate the length of the lag time.

Modelling the wind speed in the near-coastal region is subject to uncertainties, for example due to the surface roughness. Winds over land are generally weaker than winds over water due to larger surface roughness causing sustained winds to be reduced. In our model, the wind speeds at the model grid pointing closest to each of the four coastal stations were calculated using land–sea fractions (sea = 0, land = 1) of 0.27 (Blåvandshuk), 0.25 (Thyborøn), 0 (Gniben) and 0.05 (Gedser), respectively. As a result, the simulated wind speeds at the four stations were very close to those calculated from the nearest sea grid (Fig. 11). The differences in the simulated monthly mean maximum wind speeds in the neighbouring sea and land grid points at the four stations were 4.6, 4.1, 5.1 and 3.7 m s<sup>−1</sup> on average, respectively.

The monthly mean maximum wind speeds taken from instantaneous HIRHAM values were generally higher than

the maximum values derived from 10-min average readings at the land stations (Fig. 11). The RMSEs between the coupled run and observations at the four stations were 2.9, 3.2, 3.0 and 2.6 m s<sup>−1</sup>, respectively. The two simulations showed higher correlations with observations at the North Sea coast ( $\sim 0.7$ ) than in the transition area. The lowest correlation coefficient of 0.64, in the coupled simulation, was obtained at the Gniben station, which is influenced by land. The other three stations are representative for large areas under the direct influence of winds either from the North Sea or from the Baltic Sea (Lass and Matthäus, 1996).

#### 4. Discussion

One of several major issues in the development of regional coupled ocean–atmosphere models is to assess whether

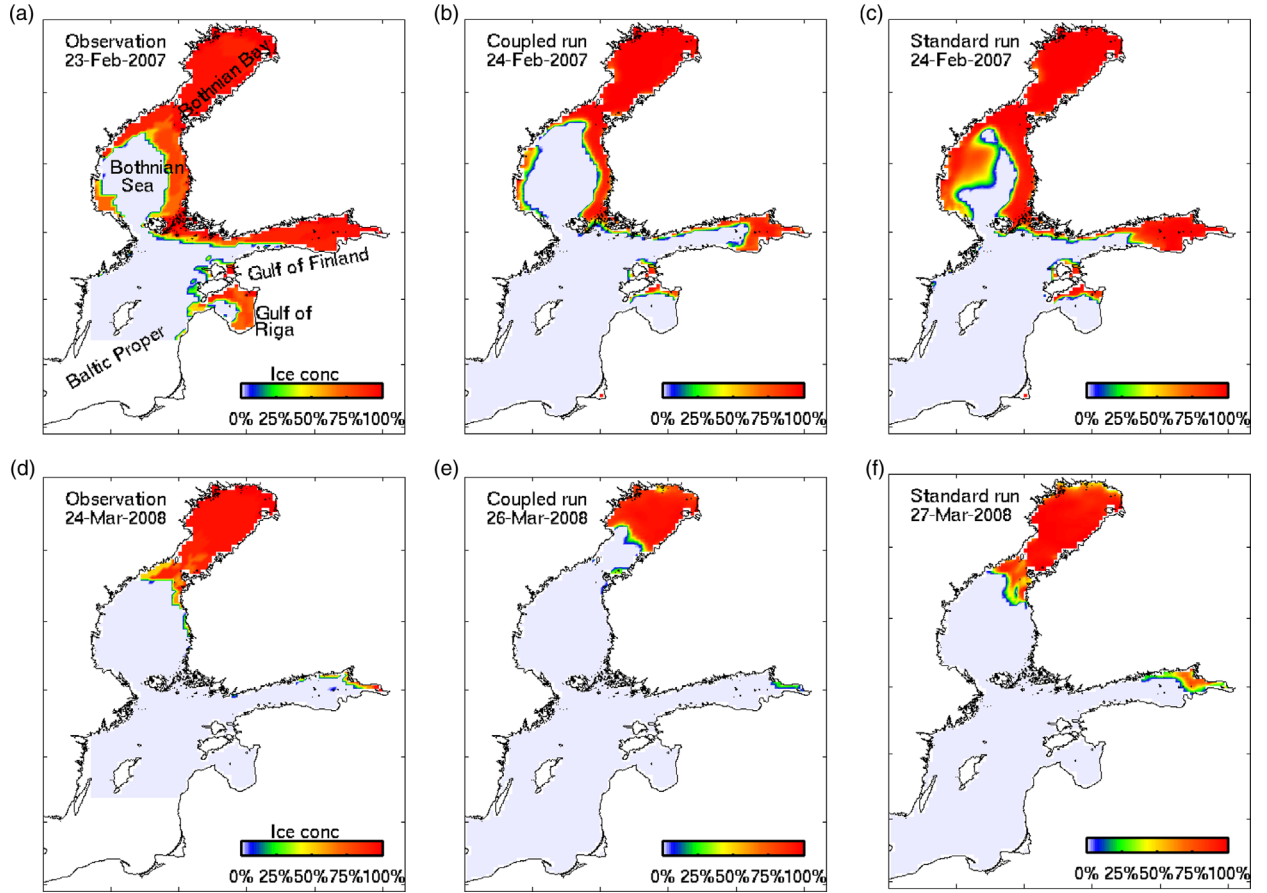


Fig. 9. Observed and modelled ice concentration distributions for the dates of MIB in the Baltic Sea in 2007 (top panels: (a)–(c)) and 2008 (bottom panels: (d)–(f)) as defined in Fig. 8. Winters 2007 and 2008 are taken as examples of an average and an extremely mild winter according to the classification by Seinä and Palosuo (1996).

coupling of the two circulation systems improves the quality of predictions of variability and extremes and whether predictive uncertainty propagates in long-term climate simulations. A common approach to evaluate RCMs is to make use of perfect boundary experiments that allow validation with respect to the statistics of the actual observed weather in the period simulated. For such experiments in hindcast mode, the driving data are so-called perfect boundary conditions, derived from global meteorological reanalyses and from compilations of observed and modelled conditions (Rummukainen, 2010). Frequently, such hindcast experiments are not performed for sufficiently long periods to investigate the model system uncertainty on multi-year time scales (Hagedorn et al., 2000; Döscher et al., 2002; Schrum et al., 2003). In contrast to previous RCM simulation studies of the Baltic Sea (Gustafsson et al., 1998; Hagedorn et al., 2000; Döscher et al., 2002; Schrum et al., 2003), this study performed two 21-yr experiments using lateral boundary conditions from the ERAI reanalysis. The quality of prescribed SSTs and sea ice data from

ERA-Interim (ERA-Interim) was evaluated against observations for the simulation period. Moreover, the present study is the first to include a two-way nested fine-grid ocean domain in the coupled RCMs. This configuration enables the ocean model to resolve water transport in the Danish straits, which is a prerequisite for a realistic simulation of baroclinic flows and of the feedback of the Baltic Sea and adjacent waters to a changing climate.

#### 4.1. Need for high-resolution models for the Baltic Sea

A climate model is better constrained towards the observed climate when SSTs and sea ice conditions are specified from observations, rather than using SSTs generated from an experiment where the model is coupled to an ocean model. For this reason, the standard simulation is considered close to the observed climate because it used perfect boundary conditions from the ERAI reanalysis. The coupled simulation has no observational constraint and hence reflects

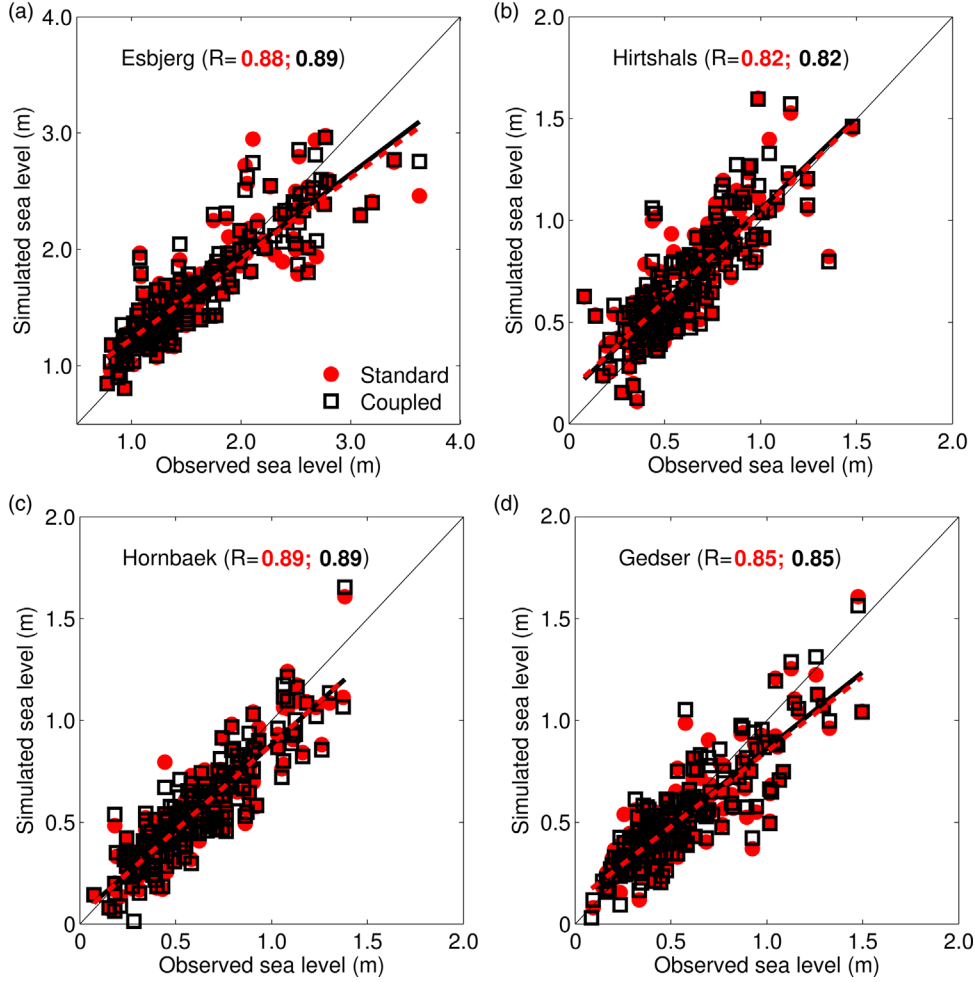


Fig. 10. Scatterplots of monthly maxima of hourly sea levels at Esbjerg, Hirtshals, Hornbæk and Gedser. Observations are plotted on the x-axis, which are retrieved from DMI tide gauges. Model results are plotted on the y-axis, indicated by black open squares (coupled) and red solid circles (standard). The correlation coefficients ( $R$ ), with  $p < 0.001$ , are given for both runs.

errors in both atmospheric forcing and the ocean model itself. Therefore, using a coupled system, there should ideally not be major deviations from the standard performance in order to have a potential for use when run in a free climate-modelling context. For the study period 1990–2010, ERAI SSTs were almost a perfect match to observations in summer but substantially overestimated sea ice distribution in the Baltic land–sea transition in winter due to the coarse resolution (Figs. 5 and 8a). The HIRHAM RCM in this high-resolution configuration tends to generate a slight warm bias in winter and a cold bias in summer in the Baltic region, probably due to model physics not being extensively tuned to the higher resolution ( $\sim 11$  km) but, rather, being taken directly from the lower resolution ( $\sim 50$  km) standard parameterisation (Christensen and Christensen, 2007). By compensating for errors in the prescribed ERAI SSTs, the standard HIRHAM simulation showed relatively low 2-m air

temperatures in winter for the Baltic Sea (Fig. 4a). Subsequently, the standard HBM simulation yielded underestimated SSTs and an overestimated ice extent. In the coupled simulation, the ocean model fitted well with the HIRHAM forcing by providing high-resolution SST fields. The winter SSTs and sea ice in the coupled simulation were in closer agreement with observations than the ERAI reanalysis and the standard simulation. However, in summer, the ocean model worked less well with a cold bias in SSTs in both simulations. In comparison with in situ measurements, the absolute values of the JJA mean differences were mostly below  $0.5^\circ\text{C}$ . For the coupled run, the JJA mean differences were somewhat amplified relative to the standard run, with absolute values below  $1^\circ\text{C}$ . Overall, we conclude that the coupled simulation without observational constraints in the Baltic Sea showed only minor deviations in air–sea interaction compared to the standard run with atmospheric boundary forcing from



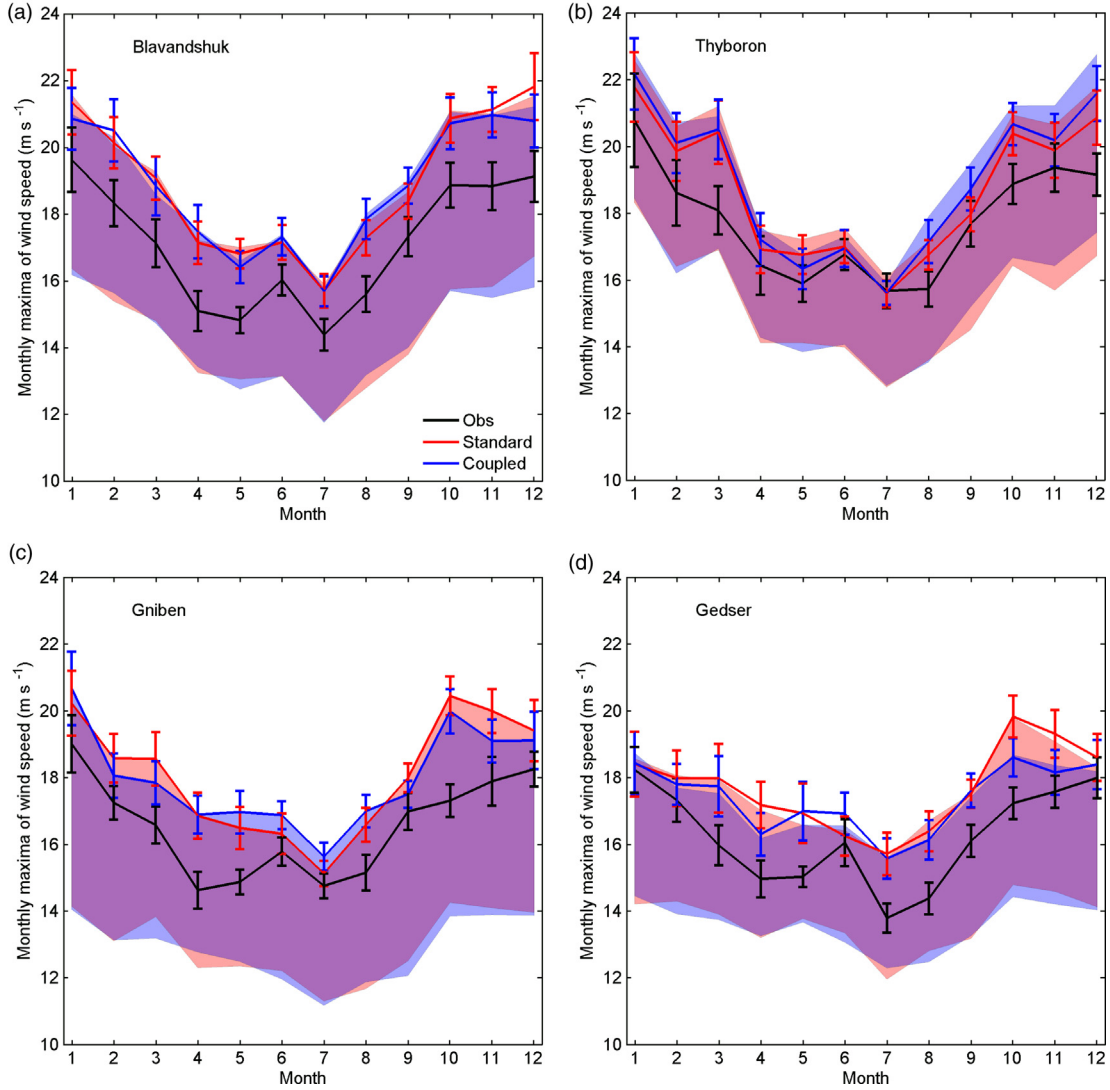


Fig. 11. Monthly mean maximum wind speeds (1990–2010) with error bars at Blavandshuk, Thyborøn, Griben and Gedser. The observations (black) are derived from continuous 10-min average readings at the DMI land stations. The modelled wind speed is taken from hourly instantaneous values at model grid points with land–sea fractions closest to the observation stations in the coupled (blue) and standard (red) simulations. Error bar indicates one standard error of the mean. The shaded areas show the model results from the sea grid (upper limit) and from the land grid (lower limit) closest to the observation stations.

ERA-Interim reanalysis. The modelled near-surface atmosphere was more sensitive to high-resolution modelled SSTs in the Baltic land–sea transition, such as the Bothnian Sea, the GF and the south Gulf of Riga (Fig. 3), with significant improvement in winter.

These simulations included a fine-grid ocean domain for the transition zone between the North Sea and Baltic Sea. This was done because bathymetry in the Danish straits is one of the governing factors for water exchange between these two regional seas (Bendtsen et al., 2009; Burchard et al., 2009). The HBM ocean model with a two-way nested fine-grid domain has been shown to effectively stress both

barotropic and baroclinic factors in the water exchange (She et al., 2007). Both the barotropic and baroclinic effects play important roles for water mass exchange and Baltic Sea circulation, especially in a long-term run (Meier and Kauker, 2003; Meier, 2006). In this simulation, the modelled annual average transport through the Danish straits matched the annual average river inflow to the Baltic Sea. On a yearly basis, the model was capable of reproducing the saline water from the transition entering the Bornholm Deep (Fig. 2). However, the model underestimated the effect of saline water inflow in the central Baltic Sea due to coarse vertical resolution. A recent study

has shown that a combination of a horizontal resolution of 1 nm and fine vertical grids is a prerequisite to simulate realistic baroclinic flows in the Western Baltic Sea (Hofmeister et al., 2011). By extending the fine-grid domain to the central Baltic Sea with 1-nm horizontal resolution and vertical finer resolution in deep basins, the HBM is capable of reproducing the salt transport and bottom salinity from the Bornholm Deep to the Gotland Deep with great accuracy (L. Jonasson, DMI, personal communication). If ocean circulation has an impact on these SST patterns, it would potentially leave an imprint on climate in the coupled system.

In this configuration, the HBM was more prone to changes in shallow waters than deep basins to the induced changes in atmospheric forcing in the coupled system (Fig. 7). An exception was found in the transition zone, where the nested fine-grid ocean model yielded a better agreement with SST measurements than the coarse-grid one did and also showed less difference in the coupled model (see Fig. 6). In turn, the atmospheric modulation induced by SSTs from the fine-grid domain was negligible. This indicates that a fine-grid domain is useful in reducing biases when modelling sea surface conditions in the feedback process. Obviously, an extended fine-grid domain including the transition zone and the central Baltic Sea has the potential to provide a more realistic description of the Baltic Sea circulation and SSTs. The adaptation of a two-way nested ocean model in a regional model is a computationally efficient way of reducing errors in the air–sea interaction and their propagation in long-term climate simulations.

For climate research at a local scale like Denmark, a small increase in storm activity and strength over Denmark and the adjacent waters is anticipated by 2100, associated with more frequent westerly winds and a slightly eastward shift of the storm tracks over the North Atlantic Ocean (IPCC, 2007; Pryor et al., 2012). In formulating a Danish strategy for adaptation to a changing climate, it is crucial to acquire knowledge of the highest sea levels reached in extreme wind storm events, in addition to an estimation of the expected global sea level rise. In the present 21-yr RCM experiments, the monthly maximum wind speeds and sea levels show minor differences between the two simulations and agree well with observations along the Danish coasts. The difference in monthly maximum wind speeds between sea grid points and land grid points at the four near-coastal stations can be up to  $5 \text{ m s}^{-1}$  on average because winds over water are generally stronger than those over land. Furthermore, the simulated wind speeds showed slightly higher correlations with the observations at the western Danish coasts than in the inner Danish waters due to winds in the latter area receiving more disturbances from the surrounding islands. This suggests a need for high-

resolution RCMs in resolving local orography, land–sea contrast and small-scale atmospheric features such as convective cells for the inner Danish waters. Given these circumstances, we conclude that the model setup presented here may be suitable for a description of changes in extreme conditions.

#### 4.2. Towards a fully coupled system in the Baltic Sea

Coupled atmospheric and ocean models have been increasingly used in regional climate-modelling studies. This is not only due to the coupling between the ocean and the atmosphere, which enables a representation of physical interactions and feedback processes, but also because a coupling can prevent RCM large-scale drift due to the biased sea surface fields in small ocean basins in global climate models (Rummukainen, 2010). Despite the presented biases in the prescribed and coupled simulations, both simulations performed reasonably well for the inter-annual variability of SST and ice extent in the Baltic Sea as well as monthly maximum sea levels and wind speeds at the Danish coasts from 1990 to 2010. We are confident that both models with the presented configurations are adequate for long-term simulations and are good candidates for further development towards a fully coupled system in the Baltic Sea and adjacent waters.

However, the coupling needs some improvements. First, a proper coupling interval should be specified according to the interaction time scales of interest in climate change research. Sensitivity experiments of SST high-frequency coupling in a GCM system show that intra-daily SST variability is negligible in the annual mean state and seasonal cycle of the tropical climate but can systematically stress the interannual variability like El Niño Southern Oscillation characteristics (Masson et al., 2012). Second, when coupling the regional ocean, the heat (and water) exchanges at the air–sea interface have to be done in a consistent way, allowing the two components to reach equilibrium. In this study, the atmosphere and ocean are not flux coupled, and hence the interface is possibly not energy conserving due to different bulk formulations in the atmospheric and ocean models. Finally, information from a coupled distributed surface runoff model has to be included in the coupled system in order to provide a consistent quantitative assessment of climate change impacts at regional and local scales.

## 5. Conclusion

We investigate the impact of atmospheric response by replacing prescribed ERAI SSTs with modelled SSTs in

the Baltic Sea and Danish coasts by coupling two independent models, HIRHAM and HBM, at a high resolution of 6 nm. Two experiments were performed for the period 1990–2010 using lateral boundary conditions from ERAI. The prescribed simulation yielded underestimation of winter SSTs and overestimation of sea ice extent in the Baltic Sea due to a large bias in the coarse-resolution ERAI data. This bias could be compensated by high-resolution modelled SSTs. Hence, the coupled simulation showed a great improvement in both winter SSTs and sea ice extent in the Baltic Sea. By contrast, the summer ERAI SSTs agreed well with observations. The prescribed simulation yielded a slight cold bias in the Baltic Sea. This bias was somewhat amplified in the coupled simulation. This could be due to a combination of errors from both atmospheric and ocean models without observational constraints. Overall, the coupled atmosphere and ocean in the Baltic coastal region exhibited higher winter means and lower summer means in 2-m air temperatures and SSTs, compared to the prescribed simulation. The absolute values of seasonal mean differences between the two simulations were below 2°C in 2-m air temperatures and below 1°C in SSTs. These minor deviations indicate that the coupled atmospheric and ocean models are stable over a seasonal cycle for a 21 yr simulation and are good candidates for further development towards a fully coupled system for longer term simulations.

The coupled system is the first to include a two-way nested fine-grid ocean domain (1-nm resolution) for the transition zone between the North Sea and Baltic Sea. The fine-grid ocean model provided better accuracy in simulating SSTs and showed smaller differences between the two simulations than the coarse-grid ocean model did. In turn, the modification on the atmosphere induced by modelled SSTs was negligible. Hence, the simulated monthly maximum wind speeds around the Danish coasts only showed minor differences between the two experiments and agreed well with observations. Previous studies have shown that a horizontal resolution of at least 1 nm is crucial for the transition zone and the central Baltic Sea to describe the water exchange between the two regional seas and realistic baroclinic flows in the Baltic Sea. Therefore, our experiments indicate that including a nested fine-grid ocean domain within RCMs is useful not only to study local climates like Danish coasts but also to prevent SST biases in the feedback process. This demonstrates a need for a fine-grid domain extending from the transition to the central Baltic Sea to reduce uncertainty in the air–sea interaction in the Baltic coastal region, where the atmosphere was relatively sensitive to modelled SSTs in this study. This work provides a first attempt to resolve the Danish coasts using high-resolution RCMs. It also serves as a knowledge basis for the development of a fully coupled system with a particular interest for the Danish coasts, as

well as for other coastal regions with similarly complex coastlines and land–sea contrasts.

## 6. Acknowledgments

This work received financial support from the Danish Strategic Research Council through its support of the Centre for Regional Change in the Earth System (CRES; [www.cres-centre.dk](http://www.cres-centre.dk)) under contract no. DSF-EnMi 09-066868, and furthermore it is part of the Greenland Climate Research Centre (project 6504). The authors thank Neil MacKellar for his early contribution to the coupling work, Kristine S. Madsen for providing sea-level data and Morten Larsen for assessing the model setup. They are also grateful to Jian Su, Jacob Woge Nielsen and Jens Murawski for comments during the process. ECMWF is acknowledged for the use of the ERAI data. The MyOcean project is also acknowledged for providing sea ice concentrations in 2007 and 2008 by Germa Väli and satellite SST data from 1990 to 2010 by Simon Jandt. They also thank the anonymous reviewer for the helpful comments, which improved this article.

## References

- BACC. 2008. *Assessment of Climate Change for the Baltic Sea Basin*. Springer, Heidelberg, Germany, 474 pp.
- Bendtsen, J., Gustafsson, K., Söderkvist, J. and Hansen, J. 2009. Ventilation of bottom water in the North Sea–Baltic Sea transition zone. *J. Mar. Syst.* **75**(1–2), 138–149.
- Berg, P. 2012. *Mixing in HBM*. DMI Scientific Report No. 12-03, ISSN: 978-87-7478-610-8, Copenhagen, 21 pp. Online at: <http://www.dmi.dk/dmi/sr12-03.pdf>
- Berg, P. and Poulsen, J. 2012. *Implementation Details for HBM*. DMI Technical Report No. 12-11, ISSN: 1399-1388, Copenhagen. Online at: <http://www.dmi.dk/dmi/tr12-11.pdf>
- Burchard, H., Janssen, F., Bolding, K., Umlauf, L. and Rennau, H. 2009. Model simulations of dense bottom currents in the Western Baltic Sea. *Cont. Shelf. Res.* **29**(1), 205–220.
- Christensen, J. and Christensen, O. 2007. A summary of the PRUDENCE model projections of changes in European climate by the end of this century. *Clim. Change* **81**, 7–30.
- Christensen, J., Kjellström, E., Giorgi, F., Lenderink, G. and Rummukainen, M. 2010. Weight assignment in regional climate models. *Clim. Res.* **44**(2), 179–194.
- Christensen, J. H. and Christensen, O. B. 2003. Severe summertime flooding in Europe. *Nature* **421**(6925), 805–806.
- Christensen, O., Drews, M., Christensen, J., Dethloff, K., Ketelsen, K. and co-authors. 2006. *The HIRHAM Regional Atmospheric Climate Model Version 5*. DMI technical report 06-17, 22 pp. Online at: <http://www.dmi.dk/dmi/tr06-17.pdf>
- Dee, D., Uppala, S., Simmons, A., Berrisford, P., Poli, P. and co-authors. 2011. The ERA-Interim reanalysis: configuration and performance of the data assimilation system. *Q. J. Roy. Meteorol. Soc.* **137**(656), 553–597.

- Döscher, R., Willén, U., Jones, C., Rutgersson, A., Meier, H. and co-authors. 2002. The development of the regional coupled ocean-atmosphere model RCAO. *Boreal. Environ. Res.* **7**(3), 183–192.
- Dumenil, L. 1992. A rainfall-runoff scheme for use in the Hamburg climate model. In: *Advances in Theoretical Hydrology* (ed. J. P. O’Kane). European Geophysical Society series of hydrological sciences 1, Elsevier, pp. 129–157.
- Eerola, K. 2006. About the performance of HIRLAM version 7.0. *Hirlam Newsletter* **51**, 93–102.
- Fu, W., She, J. and Dobrynin, M. 2012. A 20-yr reanalysis experiment in the Baltic Sea using three-dimensional variational (3DVAR) method. *Ocean. Sci.* **8**, 827–844.
- Graham, L. 1999. Modeling runoff to the Baltic Sea. *Ambio*. **28**(4), 328–334.
- Gustafsson, N., Nyberg, L. and Omstedt, A. 1998. Coupling of a high-resolution atmospheric model and an ocean model for the Baltic Sea. *Mon. Wea. Rev.* **126**(11), 2822–2846.
- Hagedorn, R., Lehmann, A. and Jacob, D. 2000. A coupled high resolution atmosphere-ocean model for the BALTEX region. *Meteorol. Z.* **9**(1), 7–20.
- Hofmeister, R., Beckers, J.-M. and Burchard, H. 2011. Realistic modelling of the exceptional inflows into the central Baltic Sea in 2003 using terrain-following coordinates. *Ocean. Model.* **39**(3), 233–247.
- Høyer, J. and She, J. 2004. *Validation of Satellite SST Products for the North Sea-Baltic Sea Region*. DMI Technical Report No. 04-11, 31 pp. Online at: <http://www.dmi.dk/dmi/tr04-11.pdf>
- IPCC. 2007. Causes of observed changes in extremes and projections of future changes. In: *Climate Change 2007: The Physical Science Basis. Contribution of Working Group I to the Fourth Assessment Report of the Intergovernmental Panel on Climate Change*. (eds. S. Solomon, D. Qin, M. Manning, Z. Chen, M. Marquis and co-authors). Cambridge University Press, Cambridge, 996 pp.
- Jacob, D., Bärring, L., Christensen, O. B., Christensen, J. H., de Castro, M. and co-authors. 2007. An inter-comparison of regional climate models for Europe: model performance in present-day climate. *Clim. Change* **81**, 31–52.
- Janssen, F., Schrum, C. and Backhaus, J. 1999. A climatological data set of temperature and salinity for the Baltic Sea and the North Sea. *Dtsch. Hydrograph. Z.* **51**, 5–245.
- Kjellström, E. and Giorgi, F. 2010. Introduction. *Clim. Res.* **44**, 117–119.
- Kleine, E. and Sklyar, S. 1995. Mathematical features of Hibler’s model of large-scale sea-ice dynamics. *Ocean. Dyn.* **47**(3), 179–230.
- Larsen, M., Thejll, P., Christensen, J., Refsgaard, J. and Jensen, K. 2013. On the role of domain characteristics in the simulations with a regional climate model. *Clim. Dyn.* **40**, 2903–2918.
- Lass, H. and Matthäus, W. 1996. On temporal wind variations forcing salt water inflows into the Baltic Sea. *Tellus A.* **48**(5), 663–671.
- Lehmann, A., Lorenz, P. and Jacob, D. 2004. Modelling the exceptional Baltic Sea inflow events in 2002–2003. *Geophys. Res. Lett.* **31**(21), L21308.
- Leppäranta, M. and Myrberg, K. 2009. *Physical Oceanography of the Baltic Sea*. Springer Praxis Publishing, Chichester, UK.
- Liu, W., Katsaros, K. and Businger, J. 1979. Bulk parameterization of air-sea exchanges of heat and water vapor including the molecular constraints at the interface. *J. Atmos. Sci.* **36**(9), 1722–1735.
- Löptien, U. and Meier, H. 2011. The influence of increasing water turbidity on the sea surface temperature in the Baltic Sea: a model sensitivity study. *J. Mar. Syst.* **88**, 323–331.
- Lucas-Picher, P., Wulff-Nielsen, M., Christensen, J., Aðalgeirsdóttir, G., Mottram, R. and co-authors. 2012. Very high resolution regional climate model simulations over Greenland: identifying added value. *J. Geophys. Res.* **117**, D02108. DOI: 10.1029/2011JD016267.
- Masson, S., Terray, P., Madec, G., Luo, J., Yamagata, T. and co-authors. 2012. Impact of intra-daily SST variability on ENSO characteristics in a coupled model. *Clim. Dyn.* **39**, 681–707.
- Meier, H. 2006. Baltic Sea climate in the late twenty-first century: a dynamical downscaling approach using two global models and two emission scenarios. *Clim. Dyn.* **27**(1), 39–68.
- Meier, H. 2007. Modeling the pathways and ages of inflowing salt- and freshwater in the Baltic Sea. *Estuarine. Coastal. Shelf. Sci.* **74**(4), 610–627.
- Meier, H. and Kauker, F. 2003. Modeling decadal variability of the Baltic Sea: 2. Role of freshwater inflow and large-scale atmospheric circulation for salinity. *J. Geophys. Res.* **108**(C11), 3368.
- Neumann, T. 2010. Climate-change effects on the Baltic Sea ecosystem: a model study. *J. Mar. Syst.* **81**(3), 213–224.
- Nordeng, T. 1994. *Extended Versions of the Convective Parameterization Scheme at ECMWF and Their Impact on the Mean and Transient Activity of the Model in the Tropics*. Technical Memorandum. 206, European Centre for Medium-Range Weather Forecasts, Reading, UK, 41 pp.
- Pezzulli, S., Stephenson, D. and Hannachi, A. 2005. The variability of seasonality. *J. Clim.* **18**, 71–88.
- Pryor, S., Barthelmie, R., Clausen, N., Drews, M., MacKellar, N. and Kjellström, E. 2012. Analyses of possible changes in intense and extreme wind speeds over northern Europe under climate change scenarios. *Clim. Dyn.* **38**(1–2), 189–208.
- Rockel, B. and Woth, K. 2007. Extremes of near-surface wind speed over Europe and their future changes as estimated from an ensemble of RCM simulations. *Clim. Change* **81**, 267–280.
- Roeckner, E., Bäuml, G., Bonaventura, L., Brokopf, R., Esch, M. and co-authors. 2003. *The Atmospheric General Circulation Model ECHAM5. Part 1. Model Description*. Report no. 349, Max-Planck-Institut für Meteorologie (MPI-M), Hamburg.
- Rummukainen, M. 2010. State-of-the-art with regional climate models. *Wiley. Interdiscip. Rev. Clim. Change* **1**(1), 82–96.
- Schrum, C., Hübner, U., Jacob, D. and Podzun, R. 2003. A coupled atmosphere/ice/ocean model for the North Sea and the Baltic Sea. *Clim. Dyn.* **21**(2), 131–151.
- Seinä, A. and Palosuo, E. 1996. The classification of the maximum annual extent of ice cover in the Baltic Sea 1720–1995. *Meri.* **27**, 79–910.
- She, J., Berg, P. and Berg, J. 2007. Bathymetry impacts on water exchange modelling through the Danish straits. *J. Mar. Syst.* **65**(1–4), 450–459.

- Sundqvist, H. 1978. A parameterization scheme for non-convective condensation including prediction of cloud water content. *Q. J. Roy. Meteorol. Soc.* **104**(441), 677–690.
- Tiedtke, M. 1989. A comprehensive mass flux scheme for cumulus parameterization in large-scale models. *Mon. Wea. Rev.* **117**(8), 1779–1800.
- Umlauf, L., Burchard, H. and Hutter, K. 2003. Extending the  $k-w$  turbulence model towards oceanic applications. *Ocean. Model.* **5**(3), 195–218.
- Vihma, T. and Haapala, J. 2009. Geophysics of sea ice in the Baltic Sea: a review. *Prog. Oceanogr.* **80**(3–4), 129–148.
- von Storch, H., Langenberg, H. and Feser, F. 2000. A spectral nudging technique for dynamical downscaling purposes. *Mon. Wea. Rev.* **128**(10), 3664–3673.
- Wan, Z., She, J., Maar, M., Jonasson, L. and Baasch-Larsen, J. 2012. Assessment of a physical-biogeochemical coupled model system for operational service in the Baltic Sea. *Ocean. Sci.* **8**, 683–701.